Performance of UWB Multiple-Access Impulse Radio Systems With Antenna Array in Dense Multipath Environments

S. S. Tan, B. Kannan, *Member, IEEE*, and A. Nallanathan, *Senior Member, IEEE*

***Abstract*—In this letter, the influence of temporal and spatial diversities on the performance of ultra-wideband time-hopping pulse-position modulated multiple-access impulse radio (IR) systems is analyzed. We investigate how an antenna array can be used at the receiver to improve the bit-error rate (BER) performance and can cope with the effects of multiple-access interference of IR system in dense multipath environments. Analytical and simulation results show that the BER performance of the IR systems can be improved when the number of array elements is increased. The performance can be further improved by coherently adding more multipaths at the receiver.**

***Index Terms*—Antenna array, impulse radio (IR), multipath, multiple access, ultra-wideband (UWB).**

I. Introduction

IMPULSE RADIO (IR) is based on an ultra-wideband (UWB) time-hopping (TH) spread-spectrum technique, in which subnanosecond pulses are modulated to convey information by shifting the relative time position of the pulses. Performance of IR under ideal propagation conditions, where there is only a single path between each user's transmitter and receiver, has been investigated in [1]. A Rake receiver can be used positively to reap the benefits of multipath diversity in UWB systems [2], [3]. Analysis on Rake-type receivers for UWB systems in dense multipath environments is discussed in [4]. The multipath characteristics of IR systems based on single-antenna reception are discussed in [5] and [6]. Antenna array is a promising approach for capacity enhancement and performance improvement in wireless systems. In dense multipath environments, antenna array can be used in conjunction with the Rake receiver to exploit the spatial and temporal diversities. This letter presents the diversity performance of the IR systems with antenna array in the presence of multipath and multiple access interference (MAI). Specifically, uniform rectangular and linear arrays with selective Rake (SRake) are employed at the receiver. Particular attention is given to the effects of the number of antenna elements and selected multipaths on the bit-error rate (BER) performance.

Paper approved by M. Z. Win, the Editor for Equalization and Diversity of the IEEE Communications Society. Manuscript received July 4, 2003; revised May 28, 2005.

S. S. Tan and A. Nallanathan are with the Department of Electrical and Computer Engineering, National University of Singapore, Singapore 119260 (e-mail: engp2444@nus.edu.sg; elena@nus.edu.sg).

B. Kannan is with the School of Surveying and Spatial Information Systems, University of New South Wales, Sydney NSW 2052, Australia.

Digital Object Identifier 10.1109/TCOMM.2006.876828

II. System Model

A. TH-PPM Signal Model

In this letter, binary IR modulation is considered. A TH pulse-position modulated (TH-PPM) signal for the uth user can be modeled as

$$s^{(u)}(t) = \sum_{j=-\infty}^{j=\infty} w\left(t - jT_f - c_j^{(u)}T_c - \delta d_j^{(u)}\right) \quad (1)$$

where $w(t)$ represents the received monocycle waveform, T_f corresponds to the frame interval, and T_c is the chip duration. In order to support multiusers, each user is assigned a distinctive TH sequence $\{c_j^{(u)}\}$. The PPM is used for bit encoding, whereby each bit is encoded by delaying the N_s pulses with an additional time shift. The data sequence $\{d_j^{(u)}\} \in \{0,1\}$ of the uth user is a binary stream that conveys the information. The modulating data symbol changes only after every N_s hops. Therefore, $d_{iN_s}^u = d_{iN_s+1}^u \cdots\cdots = d_{(i+1)N_s-1}^u = D_i^u$ for all i, where D_i^u is the ith transmitted bit, and d_j^u is the ith repeated transmitted bit in the jth frame for $j = iN_s, iN_s+1, iN_s+2, \ldots, (i+1)N_s - 1$.

B. Antenna-Array Geometry and its Parameters

In this letter, we consider uniform rectangular $(R_x = M \times N)$ and linear $(R_x = M \times 1)$ arrays at the receiver. The beamformer output for an array steered towards an azimuth angle of ϕ and an elevation angle of θ on the incidence of a plane wave from an azimuth angle of ϕ_0 and an elevation angle of θ_0 is defined as [7]

$$B(\phi,\theta,t) = \sum_{m=0}^{M-1}\sum_{n=0}^{N-1} a_{m,n}(\phi,\theta) \times w(t - \tau_{m,n}) \quad (2)$$

where $a_{m,n}(\phi,\theta)$ is the pattern of the (m,n)th antenna element, and $\tau_{m,n}$ is the time delay of the received signal at the (m,n)th element, which is measured with respect to the reference element (M_c, N_c), is given by

$$\tau_{m,n} = \left[(M_c - m)\frac{d_x}{c}(u - u_0)\right] + \left[(n - N_c)\frac{d_y}{c}(v - v_0)\right]. \quad (3)$$

In (3), $u = \sin\phi\sin\theta$, $u_0 = \sin\phi_0\sin\theta_0$, $v = \cos\phi\sin\theta$, $v_0 = \cos\phi_0\sin\theta_0$, and c is the speed of light. The spacing between the antenna elements in x and y directions are denoted by d_x and d_y, respectively. The antenna elements are equally spaced, where $d_x = d_y = 6''$. We assume that the signals are on the xy plane, and hence, the elevation angle, $\theta = 90°$. The

channel model used in this letter is similar to the one described in [8] and [9], which is also the recommended channel model of IEEE 802.15.3a.

III. Receiver Processing

Consider an antenna array with $(R_x = M \times N)$ antenna elements. Each and every element is equipped with an SRake with L_f-Rake fingers. Without loss of generality, we assume that the receiver is perfectly synchronized to the hopping sequence of the desired user (user 1), the delays and channel coefficients of the selected paths are known at the receiver, and the receiver selects $L_f^{u=1}$ dominant paths of user 1. Besides, the time delay between the desired user and each interference user is uniformly distributed. The received signal can be written as (4) where $n_{si}(t)$ is the self-interference (SI), $n_{\text{mai}}(t)$ is the MAI, and $n_{m,n}(t)$ is the additive white Gaussian noise (AWGN) at the (m,n)th element with double-sided power spectral density of $N_0/2$. In (4), $\alpha^u_{l,m,n}$ is the channel gain of the lth path at the (m,n)th antenna element for the uth user, and $\tau^u_{l,m,n}$ is the time delay of the lth path at the (m,n)th element for the uth user. Without loss of generality, we assume $\tau^1_{0,M_c,N_c} = 0$. The total number of multipath for the uth user is denoted by L^u_{total}

$$\begin{aligned} r(t) = &\sum_{m=0}^{M-1}\sum_{n=0}^{N-1}\sum_{l_f=0}^{L_f^1-1}\alpha^1_{l_f,m,n}s^1\left(t-\tau^1_{l_f,m,n}\right) \\ &+\underbrace{\sum_{m=0}^{M-1}\sum_{n=0}^{N-1}\sum_{l=L_f^1}^{L^1_{\text{total}}-1}\alpha^1_{l,m,n}s^1\left(t-\tau^1_{l,m,n}\right)}_{n_{\text{si}}(t)} \\ &+\underbrace{\sum_{u=2}^{N_u}\sum_{m=0}^{M-1}\sum_{n=0}^{N-1}\sum_{l=0}^{L^u_{\text{total}}-1}\alpha^u_{l,m,n}s^u\left(t-\tau^u_{l,m,n}\right)}_{n_{\text{mai}}(t)} \\ &+\sum_{m=0}^{M-1}\sum_{n=0}^{N-1}\eta_{m,n}(t). \end{aligned} \tag{4}$$

The received signal is correlated with the correspondent template waveform at each finger of every antenna element, followed by sampling and summation. Thus, the correlator output at the l_fth finger of the (m,n)th element during the ith symbol period is given by (5), shown at the bottom of the page, where v_{bit} is the template signal for one bit duration, and is defined as

$$\begin{aligned} v_{\text{bit}}(t) &= \sum_{j=iN_s}^{(i+1)N_s-1} v\left(t-jT_f-c_j^1T_c-\tau^1_{l_f,m,n}\right) \\ &= w_{\text{bit}}(t)-w_{\text{bit}}(t-\delta). \end{aligned} \tag{6}$$

The bit waveform $w_{\text{bit}}(t)$ in (6) is defined as

$$w_{\text{bit}}(t) = \sum_{j=iN_s}^{(i+1)N_s-1} w\left(t-jT_f-c_j^1T_c-\tau^1_{l_f,m,n}\right). \tag{7}$$

The test statistics of the ith transmitted symbol $G(i)$ depends on the sum of the pulse correlator outputs of each selected path of each antenna element, and is given by (8), shown at the bottom of the next page. The noise term N_{total} in (8) is the summation of the total SI (I_{si}), MAI (I_{mai}), and AWGN (η) at the receiver output. The receiver makes binary decisions based on the test statistics as shown in

$$\begin{aligned} G(i) \geq 0 &\Rightarrow D_i^1 = 0 \\ G(i) < 0 &\Rightarrow D_i^1 = 1. \end{aligned} \tag{9}$$

IV. BER Analysis

Assuming that the channel coefficients remain constant during one symbol duration, the total desired signal energy contained in all selected paths from all antenna elements is given by

$$E_s = S_T^2 = \left(\sum_{m=0}^{M-1}\sum_{n=0}^{N-1}\sum_{l_f=0}^{L_f^1-1}\left(\alpha^1_{l_f,m,n}\right)^2\right)^2 N_s^2R_{wv}^2(0) \tag{10}$$

where $R_{wv}(\tau) = \int_{-\infty}^{\infty} w(t-\tau)v(t)dt$.

$$\begin{aligned} G_{l_f,m,n}(i) &= \underbrace{\int_{t=iN_sT_f+\tau^1_{l_f,m,n}}^{(i+1)N_sT_f+\tau^1_{l_f,m,n}}\left[\alpha^1_{l_f,m,n}s^1\left(t-\tau^1_{l_f,m,n}\right)\right]\alpha^1_{l_f,m,n}v_{\text{bit}}(t)dt}_{Sd_{l_f,m,n}} + Ns_{l_f,m,n} + Nm_{l_f,m,n} + Na_{l_f,m,n} \\ Ns_{l_f,m,n} &= \int_{t=iN_sT_f+\tau^1_{l_f,m,n}}^{(i+1)N_sT_f+\tau^1_{l_f,m,n}}\left[\sum_{l=0,l\neq l_f}^{L^1_{\text{total}}-1}\alpha^1_{l,m,n}s^1\left(t-\tau^1_{l,m,n}\right)\right]\alpha^1_{l_f,m,n}v_{\text{bit}}(t)dt \\ Nm_{l_f,m,n} &= \int_{t=iN_sT_f+\tau^1_{l_f,m,n}}^{(i+1)N_sT_f+\tau^1_{l_f,m,n}}\left[\sum_{u=2}^{N_u}\sum_{l=0}^{L^u_{\text{total}}-1}\alpha^u_{l,m,n}s^u(t-\tau^u_{l,m,n})\right]\alpha^1_{l_f,m,n}v_{\text{bit}}(t)dt \\ Na_{l_f,m,n} &= \int_{t=iN_sT_f+\tau^1_{l_f,m,n}}^{(i+1)N_sT_f+\tau^1_{l_f,m,n}}\left[(\eta_{m,n}(t))\right]\alpha^1_{l_f,m,n}v_{\text{bit}}(t)dt \end{aligned} \tag{5}$$

Transmission time difference between the selected l_fth path of user 1 for the (m,n)th element and the other paths from the same user or the other active users is defined as $\tau^u_{b,(m,n)} - \tau^1_{l_f,(m,n)} = j^u_{b,l_f,(m,n)}T_f + \Delta^u_{b,l_f,(m,n)}$, where $j^u_{b,l_f,(m,n)}$ is the value of time uncertainty rounded to the nearest integer, and $\Delta^u_{b,l_f,(m,n)}$ is the error in this rounding process which is uniformly distributed over $[-T_f/2, T_f/2]$.

In this letter, we assume that the number of users and the number of multipaths are sufficiently large. Hence, by using the central limit theorem (CLT), I_{mai} and I_{si} in (8) can be modeled as Gaussian random variables. Furthermore, I_{mai} and I_{si} can be considered as independent random variables as the user signals are all assumed to be independently generated. Therefore, N_{total} can be modeled by a Gaussian random variable with zero mean and σ^2_{total} variance, where $\sigma^2_{\text{total}} = \sigma^2_{\text{si}} + \sigma^2_{\text{mai}} + \sigma^2_\eta$. The notations σ^2_{si}, σ^2_{mai}, and σ^2_η are the variances of the decision variable caused by SI, MAI, and AWGN, respectively.

The overall AWGN noise at the receiver output, η, which is defined in (8), has zero mean and its variance can be written as

$$\sigma^2_\eta = \frac{N_0}{2}\left(\sum_{m=0}^{M-1}\sum_{n=0}^{N-1}\sum_{l_f=0}^{L^1_f-1}\left(\alpha^1_{l_f,m,n}\right)^2\right)\int_{-\infty}^{\infty} v^2_{\text{bit}}(t)dt. \quad (11)$$

The variance of zero-mean MAI at the receiver output is given by

$$\sigma^2_{\text{mai}} = \frac{N_s}{T_f}\sum_{m=0}^{M-1}\sum_{n=0}^{N-1}\sum_{l_f=0}^{L^1_f-1}\sum_{u=2}^{N_u}\sum_{l=0}^{L^u_{\text{total}}-1}\left(\alpha^1_{l_f,m,n}\alpha^u_{l,m,n}\right)^2 \times \int_{-\infty}^{\infty} R^2_{wv}(x)dx. \quad (12)$$

Similarly, we can show that the SI has zero mean and its variance is

$$\sigma^2_{\text{si}} = \frac{N_s}{T_f}\sum_{m=0}^{M-1}\sum_{n=0}^{N-1}\sum_{l_f=0}^{L^1_f-1}\sum_{\substack{l=0\\ l\neq l_f}}^{L^1_{\text{total}}-1}\left(\alpha^1_{l_f,m,n}\alpha^1_{l,m,n}\right)^2 \times \int_{-\infty}^{\infty} R^2_{wv}(x)dx. \quad (13)$$

The probability of error with MAI and SI conditioned on a particular instantaneous signal-to-interference-plus-noise (SINR) per bit can be written as

$$P_{E/\gamma_b} = Q\left(\sqrt{\frac{E_s}{\sigma^2_{\text{si}} + \sigma^2_{\text{mai}} + \sigma^2_\eta}}\right). \quad (14)$$

The average bit-error probability in the presence of fading, P_E, is computed using Monte Carlo method, where

$$P_E = (1/Z)\sum_{i=1}^{Z} P_{E/\gamma_b,i}. \quad (15)$$

In (15), Z is the number of channel realizations, which is taken as 10 000.

V. Numerical Results

We select the Gaussian monocycle pulse shape to be

$$w(t) = \sqrt{\frac{8}{3\times\tau_w\times N_s}} \times\left(\left[1-4\pi\left(\frac{t-t_d}{\tau_w}\right)^2\right]\exp\left[-2\pi\left(\frac{t-t_d}{\tau_w}\right)^2\right]\right) \quad (16)$$

in which N_s pulses represent one bit, whose energy is normalized to one. In (16), $t_d = 0.25$ ns corresponds to the location of the pulse center, and $\tau_w = 0.2055$ ns determines the width of the pulse. The monocycle duration is $T_w = 0.5$ ns. The system parameters are as follows: $N_s = 8$ frames, $T_f = 50$ ns, $\delta = 0.1114$ ns, $T_c = 1$ ns, and $L^u_{\text{total}} = L_{\text{total}} = 20$. The angles of arrival of the signals at all antenna elements are assumed to be the same where $\phi = 15°$, $\phi_0 = 45°$, and $\theta_0 = 90°$. The parameters for the channel model are taken as: cluster decay factor $\Gamma = 24$, ray decay factor $\gamma = 12$, $\sigma_{\text{cluster}} = \sigma_{\text{ray}} = 3.3941$ dB. The constant ray and cluster arrival rate are assumed to be 0.5 and 0.1 ns, respectively.

Fig. 1 illustrates the theoretical and simulation results of the system's BER performance for different numbers of antenna elements and selected paths for $N_u = 50$ users. The results in this figure show that the performance of a UWB system can be improved by increasing the number of Rake fingers and/or

$$G(i) = \sum_{m=0}^{M-1}\sum_{n=0}^{N-1}\sum_{l_f=0}^{L^1_f-1} G_{l_f,m,n}(i)$$
$$= \underbrace{\sum_{m=0}^{M-1}\sum_{n=0}^{N-1}\sum_{l_f=0}^{L^1_f-1} Sd_{l_f,m,n}}_{S_T} + \overbrace{\underbrace{\sum_{m=0}^{M-1}\sum_{n=0}^{N-1}\sum_{l_f=0}^{L^1_f-1} Ns_{l_f,m,n}}_{I_{\text{si}}} + \underbrace{\sum_{m=0}^{M-1}\sum_{n=0}^{N-1}\sum_{l_f=0}^{L^1_f-1} Nm_{l_f,m,n}}_{I_{\text{mai}}} + \underbrace{\sum_{m=0}^{M-1}\sum_{n=0}^{N-1}\sum_{l_f=0}^{L^1_f-1} Na_{l_f,m,n}}_{\eta}}^{N_{\text{total}}} \quad (8)$$

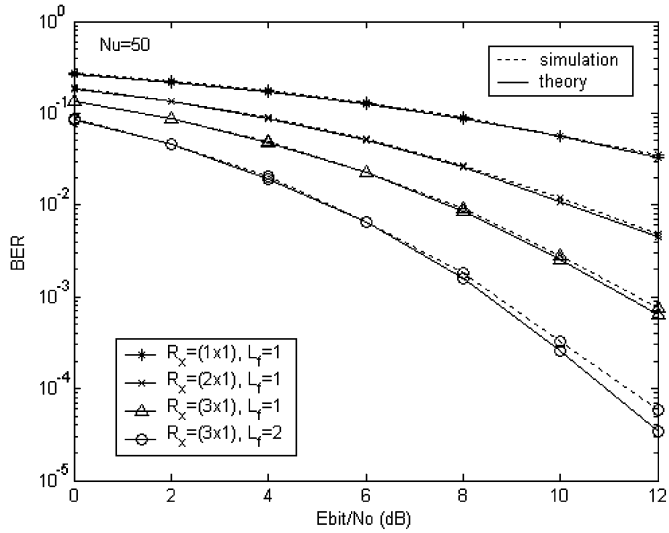

Fig. 1. BER versus $E_{\rm bit}/N_0$ for different numbers of antenna elements and selected paths.

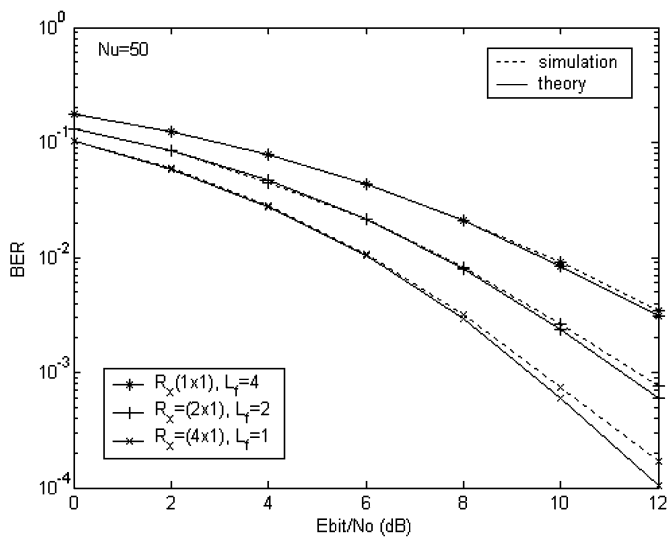

Fig. 2. Tradeoff between the number of Rake fingers and the size of antenna array.

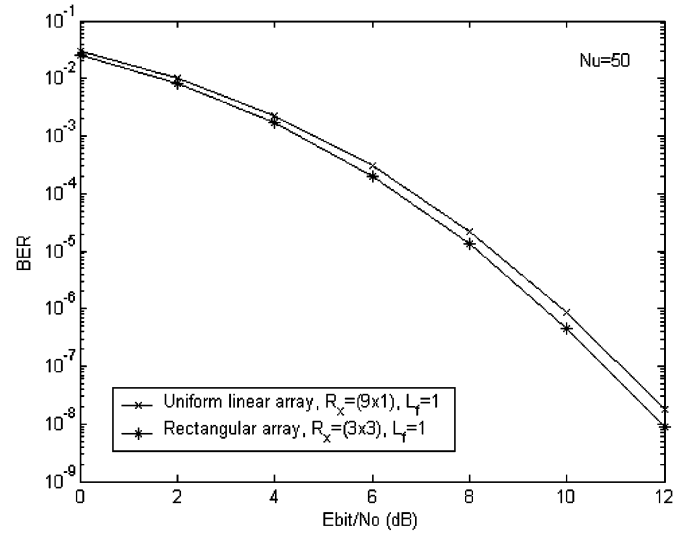

Fig. 3. Comparison between rectangular array and uniform linear array.

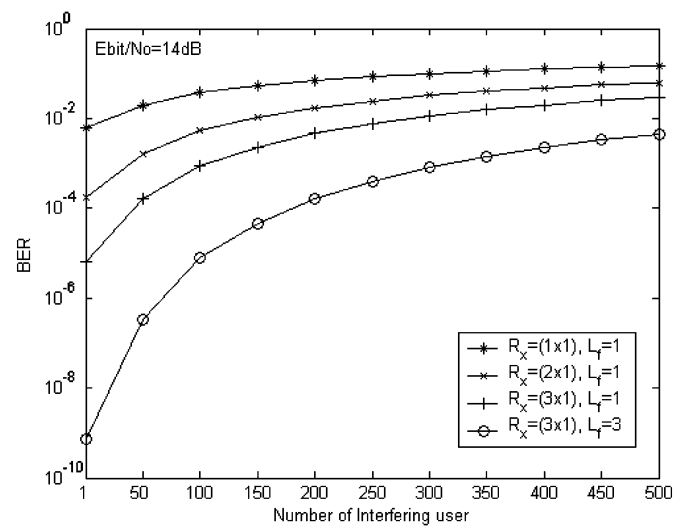

Fig. 4. BER versus number of interfering users, $N_I(= N_u - 1)$.

the array size. This improvement is due to the fact that the total energy captured by the receiver increases when the number of Rake fingers and/or the array size is increased.

In Fig. 2, we compare the tradeoff between the number of the Rake fingers and the antenna array size in a 50-user environment. In this letter, the total number of collected paths by the antenna array is kept at a constant value, and the BER performance of the system is evaluated for different array sizes. This figure shows that a system with a higher array size gives better performance. This result also demonstrates that the performance improvement from spatial diversity is greater than that from the path diversity.

In Fig. 3, with $N_u = 50$, we compare the performance of rectangular and uniform linear arrays. The results show that the BER performance of rectangular array is greater than that of the uniform linear array. This observation can be attributed to the geometry of the array. Compared with a uniform linear array, the rectangular array is capable of capturing multipath components with shorter propagation delays. Hence, the captured energy from the received multipath signals is higher than that of the uniform linear array.

Fig. 4 presents the BER performance as a function of number of interference users $N_I(= N_u - 1)$ for different numbers of antenna elements and selected paths. This result demonstrates that the system with a higher number of array elements and/or Rake fingers has greater tolerance to MAI and can support a higher number of users.

VI. Conclusions

The diversity performance of an IR multiple-access system by employing antenna array with SRake in an indoor multipath channel is presented. Antenna arrays can be used to exploit spatial diversity in conjunction with the path diversity provided by the Rake receiver to capture more energy from multipaths and improve the performance of the system. The results indicate that the BER performance of the system improves when the number

of antenna elements and/or selected multipaths increases. We have also shown that the performance improvement from spatial diversity is considerably greater than that from the path diversity. Furthermore, we also studied the impact of array geometry on the system performance. The results showed that a rectangular array can offer better performance than a uniform linear array, as the energy captured by a rectangular array is higher than that of a uniform linear array.

REFERENCES

[1] M. Z. Win and R. A. Scholtz, "Ultra-wide bandwidth time-hopping spread-spectrum impulse radio for wireless multiple-access communications," *IEEE Trans. Commun.*, vol. 48, no. 4, pp. 679–691, Apr. 2000.

[2] T. Q. S. Quek and M. Z. Win, "Analysis of UWB transmitted reference communication systems in dense multipath channels," *IEEE J. Sel. Areas Commun.*, vol. 23, no. 9, pp. 1863–1874, Sep. 2005.

[3] W. Suwansantisuk, M. Z. Win, and L. A. Shepp, "On the performance of wide-bandwidth signal acquisition in dense multipath channels," *IEEE Trans. Veh. Technol.*, vol. 54, no. 5, pp. 1584–1594, Sep. 2005.

[4] M. Z. Win and R. A. Scholtz, "Characterization of ultra-wide bandwidth wireless indoor channels: A communication-theoretic view," *IEEE J. Sel. Areas Commun.*, vol. 20, no. 9, pp. 1613–1627, Dec. 2002.

[5] M. Z. Win and R. A. Scholtz, "On the energy capture of ultra-wide bandwidth signals in dense multipath environments," *IEEE Commun. Lett.*, vol. 2, no. 9, pp. 245–247, Sep. 1998.

[6] ——, "On the robustness of ultra-wide bandwidth signals in dense multipath environments," *IEEE Commun. Lett.*, vol. 2, no. 2, pp. 51–53, Feb. 1998.

[7] R. J. Cramer, R. A. Scholtz, and M. Z. Win, "An evaluation of the ultra-wideband propagation channel," *IEEE Trans. Antennas Propagat.*, vol. 50, no. 5, pp. 561–570, May 2002.

[8] C.-C. Chong and S. K. Yong, "A generic statistical-based UWB channel for high-rise apartments," *IEEE Trans. Antennas Propagat.*, vol. 53, no. 8, pp. 2389–2399, Aug. 2005.

[9] D. Cassioli, M. Z. Win, and A. F. Molisch, "The ultra-wide bandwidth indoor channel: From statistical model to simulations," *IEEE J. Sel. Areas Commun.*, vol. 20, no. 6, pp. 1247–1257, Aug. 2002.